CSIRO PUBLISHING www.publish.csiro.au/journals/eg Copublished paper, please cite all three:
Exploration Geophysics, 2009, **40**, 154–162; *Butsuri-Tansa*, 2009, **62**, 154–162; *Mulli-Tamsa*, 2009, **12**, 154–162

A comparative study of borehole size and tool effect on dispersion curves

Weijun Zhao[1] Jongman Kim[2] Yeonghwa Kim[2,3]

[1]Centre for Northeast Asian Studies, Tohoku University, Japan.
[2]Department of Geophysics, Kangwon National University, South Korea.
[3]Corresponding author. Email: yhkim@kangwon.ac.kr

Abstract. Sonic wave dispersion characteristics are one of the most important targets of study, particularly in estimating shear wave velocity from borehole sonic logging. We have tested dispersion characteristics using monopole and dipole sources. Theoretical dispersion curves were computed for tool-absent and tool-included models having the same physical properties but different diameters (including Φ520 mm, Φ150 mm, and Φ76 mm). Comparisons were made between boreholes of different sizes and between tool-absent and tool-included models. Between the tool-included and the tool-absent boreholes, a close similarity in dispersion curve shape was revealed for the monopole source, and a significant difference was shown for the dipole source. However, for the cut-off frequency, particularly in the engineering boreholes (Φ76 mm and Φ50 mm), a significant difference was observed for signals from the monopole source, but approximately the same cut-off frequencies were found with the dipole source. This indicates the need of careful choice of source frequency in monopole-source sonic logging, particularly in an engineering borehole.

The results of numerical experiments show that cut-off frequency is exponentially proportional to the inverse of borehole radius, irrespective of the mode type and the presence of a tool, and that the cut-off frequencies for each borehole environment could be expressed as an exponential function, rather than the inversely proportional relationship between the cut-off frequency and the borehole radius that was previously generally recognised. From the direct comparison of dispersion curves, the effects on the dispersion characteristics of borehole size and the presence of the tool can be revealed more clearly than in previous studies, which presented the dispersion curve and/or characteristics for each borehole environment separately.

Key words: borehole size, cut-off frequency, dispersion, monopole and dipole source, tool effect.

Introduction

The dispersion characteristics of sonic signals have been one of the most important targets of studies in borehole sonic logs (Biot, 1952; Cheng and Toksöz, 1981; Paillet and White, 1982; Kurkjian and Chang, 1986; Rao et al., 2002; Sinha and Asvadurov, 2004) as the dispersion characteristics play a key role in sonic data acquisition and in estimating shear wave velocity from multipole sources. Dispersion properties are governed by the physical parameters of the formation and the borehole fluid. The size of the borehole and the existence of a tool within the borehole fluid are also key controlling factors in determining dispersion characteristics. Frequently in theoretical model studies, dispersion characteristics are studied under the assumption that the tool effect can be ignored, and that sonic logs rely on formation refracted arrivals and appropriate modal arrivals such as pseudo-Rayleigh, Stoneley, and flexural waves (Paillet and Cheng, 1991). However in real acoustic logging practice, the presence of additional modes such as the tool flexural mode is expected from the introduction of a downhole tool into the borehole fluid in a formation (Rao et al., 1999). The presence of a tool in the borehole is expected to make shear logging processing and interpretation more complex, particularly in a small borehole such as those mainly used for engineering or geotechnical purposes (hereinafter 'engineering boreholes').

When the effect of a tool is considered, it is useful to understand the characteristics of the three constituent parts: (a) a water-filled borehole in an infinite formation; (b) a tool in infinite water; (c) a tool in a water-filled borehole in an infinite formation (Hsu and Sinha, 1998). Borehole flexural and tool flexural modes are excited in (a) and (b), respectively, and these two modes are referred to as uncoupled modes since they are present in two completely independent systems and are measured separately. The excitation in case (c) is referred to as a coupled mode, because it consists of two propagating modes coexisting in the combined tool and borehole system (Hsu and Sinha, 1998).

In this study, dispersion curves were computed theoretically from the fluid-filled borehole in an infinite solid formation (hereinafter 'tool-absent borehole') and the borehole system with a cylindrical tool immersed in the fluid in an infinite formation (hereinafter 'tool-included borehole'). The computation of dispersion curves was carried out in the same manner as in the previous studies (Paillet and White, 1982; Hsu and Sinha, 1998; and Rao et al., 1999), but an emphasis was placed on the comparison of dispersion properties between many different borehole sizes, while keeping other borehole parameters constant. Comparisons and analyses were made between tool-absent and tool-included borehole models with different borehole sizes, with monopole and dipole sources. The effect of a tool was simulated by the insertion of a steel rod in the centre of the borehole.

 10.1071/EG08116 0812-3985/09/010154

Derivation of dispersion curves for tool-absent and tool-included boreholes

According to scalar wave-motion equations (Aki and Richards, 1980), the three displacement potentials in each cylindrical solid formation are given by

$$\begin{aligned}\Phi_j &= \left[c_{p-}^{(j)} I_n(p_j r) + c_{p+}^{(j)} K_n(p_j r)\right]\cos(n\theta)e^{i(kz-\omega t)}\\ \psi_j &= \left[c_{sh-}^{(j)} I_n(s_j r) + c_{sh+}^{(j)} K_n(s_j r)\right]\sin(n\theta)e^{i(kz-\omega t)}\\ \chi_j &= \left[c_{sv-}^{(j)} I_n(s_j r) + c_{sv+}^{(j)} K_n(s_j r)\right]\cos(n\theta)e^{i(kz-\omega t)},\end{aligned} \tag{1}$$

where j denotes the layer index, and n denotes the multipole order. $c_{p-}^{(j)}$, $c_{p+}^{(j)}$, $c_{sh-}^{(j)}$, $c_{sh+}^{(j)}$, $c_{sv-}^{(j)}$, and $c_{sv+}^{(j)}$ are unknown amplitude coefficients. $I_n(x)$ and $K_n(x)$ denote the modified Bessel functions of the first kind and the second kind of order n, respectively. The radial compressional wave number p_j and the radial shear wave number s_j satisfy the relationships

$$p_j = \sqrt{k^2 - \omega^2/\alpha_j^2} \quad \text{and} \quad s_j = \sqrt{k^2 - \omega^2/\beta_j^2}, \tag{2}$$

respectively. Because there is no incoming wave in the outmost formation, the terms associated with the amplitude coefficients $c_{p-}^{(j)}$, $c_{sh-}^{(j)}$, and $c_{sv-}^{(j)}$ are discarded.

In the tool-included fluid-filled borehole, the layer index j is 1 for the tool, 2 for the annular inviscid fluid, and 3 for the infinite homogeneous elastic formation. So, the displacement potentials in three cylindrical layers are given by

$$\begin{aligned}\phi_1 &= c_{p-}^{(1)} I_n(p_1 r)\cos(n\theta)e^{i(kz-\omega t)}\\ \psi_1 &= c_{sh-}^{(1)} I_n(s_1 r)\sin(n\theta)e^{i(kz-\omega t)}\\ \chi_1 &= c_{sv-}^{(1)} I_n(s_1 r)\cos(n\theta)e^{i(kz-\omega t)}\\ \phi_2 &= \left[c_{p-}^{(2)} J_n(p_2 r) + c_{p+}^{(2)} Y_n(p_2 r)\right]\cos(n\theta)e^{i(kz-\omega t)}\\ \phi_3 &= c_{p-}^{(3)} K_n(p_3 r)\cos(n\theta)e^{i(kz-\omega t)}\\ \psi_3 &= c_{sh}^{(3)} K_n(s_3 r)\sin(n\theta)e^{i(kz-\omega t)}\\ \chi_3 &= c_{sv+}^{(3)} K_n(s_3 r)\cos(n\theta)e^{i(kz-\omega t)}\end{aligned} \tag{3}$$

where J_n and Y_n are the Bessel functions of the first and the second of order n, respectively.

There are eight unknown amplitude coefficients in the displacement potentials expressions. In order to solve for them, boundary conditions are specified on the two cylindrical interfaces (tool-fluid and fluid-formation interfaces), and are given by

$$\begin{bmatrix} ru^{(1)} \\ \dfrac{r^2\sigma_{rr}^{(1)}}{2\mu^{(1)}} \\ \dfrac{r^2\sigma_{r\theta}^{(1)}}{2\mu^{(1)}} \\ \dfrac{r^2\sigma_{rz}^{(1)}}{\mu^{(1)}k} \end{bmatrix} = \begin{bmatrix} ru^{(2)} \\ \dfrac{r^2\sigma_{rr}^{(2)}}{2\mu^{(1)}} \\ 0 \\ 0 \end{bmatrix} \quad \text{at } r = r_1 \tag{4a}$$

and

$$\begin{bmatrix} ru^{(2)} \\ \dfrac{r^2\sigma_{rr}^{(2)}}{2\mu^{(3)}} \\ 0 \\ 0 \end{bmatrix} = \begin{bmatrix} ru^{(3)} \\ \dfrac{r^2\sigma_{rr}^{(3)}}{2\mu^{(3)}} \\ \dfrac{r^2\sigma_{r\theta}^{(3)}}{2\mu^{(3)}} \\ \dfrac{r\sigma_{rz}^{(3)}}{\mu^{(3)}k} \end{bmatrix} \quad \text{at } r = r_2. \tag{4b}$$

Rearrangement of the above equations yields the matrix $\mathbf{E}$:

$$\mathbf{E} = \begin{pmatrix} e_{11} & e_{12} & e_{13} & e_{14} & e_{15} & 0 & 0 & 0 \\ e_{21} & e_{22} & e_{23} & e_{24} & e_{25} & 0 & 0 & 0 \\ e_{31} & e_{32} & e_{33} & 0 & 0 & 0 & 0 & 0 \\ e_{41} & e_{42} & e_{43} & 0 & 0 & 0 & 0 & 0 \\ 0 & 0 & 0 & e_{54} & e_{55} & e_{56} & e_{57} & e_{58} \\ 0 & 0 & 0 & e_{64} & e_{65} & e_{66} & e_{67} & e_{68} \\ 0 & 0 & 0 & 0 & 0 & e_{76} & e_{77} & e_{78} \\ 0 & 0 & 0 & 0 & 0 & e_{86} & e_{87} & e_{88} \end{pmatrix} \begin{pmatrix} c_{p-}^{(1)} \\ c_{sh-}^{(1)} \\ c_{sv-}^{(1)} \\ c_{p-}^{(2)} \\ c_{p+}^{(2)} \\ c_{p+}^{(3)} \\ c_{sh+}^{(3)} \\ c_{sv+}^{(3)} \end{pmatrix} \tag{5}$$

In the case of the tool-absent borehole model, $\mathbf{E}$ is reduced to

$$\mathbf{E} = \begin{pmatrix} e_{54} & e_{56} & e_{57} & e_{58} \\ e_{64} & e_{66} & e_{67} & e_{68} \\ 0 & e_{76} & e_{77} & e_{78} \\ 0 & e_{86} & e_{87} & e_{88} \end{pmatrix} \begin{bmatrix} c_{p-}^{(2)} \\ c_{p+}^{(3)} \\ c_{sh+}^{(3)} \\ c_{sv+}^{(3)} \end{bmatrix} \tag{6}$$

Explicit expressions for the elements of the $\mathbf{E}$ matrix are presented by Zhao (2008). For non-trivial solutions of the matrix equation, the determinant of matrix $\mathbf{E}$ must be set to be zero, and the roots of the resulting period equation can be tracked in the frequency range of interest. The period equation for a fluid-filled borehole with a tool is represented by

$$f(\omega, k|\alpha_1, \alpha_2, \alpha_3, \beta_1, \beta_3, \rho_2/\rho_1, \rho_2/\rho_3, r_1, r_2) = 0. \tag{7a}$$

The period equation for a fluid-filled borehole without a tool is represented by

$$f(\omega, k|\alpha_1, \alpha_2, \beta_2, \rho_1/\rho_2, r_2) = 0. \tag{7b}$$

Roots of the period equations can be tracked using the bisection method, after which the phase (V_{PH}) and group (V_{GR}) velocities can be obtained by

$$V_{PH} = \frac{\omega}{k} \tag{8}$$

and

$$V_{GR} = \frac{d\omega}{dk} = -\frac{\partial f/\partial k}{\partial f/\partial \omega}. \tag{9}$$

More detailed descriptions of the derivation of dispersion curves for cylindrically layered borehole models can be found in Zhao (2008).

Borehole models

In order to simulate the tool-included borehole condition, a borehole model with a steel rod in the borehole fluid in the

infinite isotropic formation was considered, as shown in Figure 1. The symbols r_1 and r_2 denote the radii of the tool and the borehole, respectively, and α and β represent the compressional and shear velocities in the formation, respectively. Subscripts 1, 2, and 3 following the symbols α, β, and ρ are for the tool, the fluid and the formation, respectively. The tool-absent model can be achieved by excluding the tool parameters that have subscript 1 (that is, r_1, α_1, β_1, and ρ_1).

For this study, three theoretical borehole models were set up, with diameters of 76 mm, 150 mm, and 520 mm, and identical physical parameters in terms of tool, fluid, and formation. Hereinafter these will be referred to as Φ76 mm, Φ150 mm and Φ520 mm boreholes, respectively. The physical parameters of the tool, the fluid, and the formation for the theoretical model boreholes were determined from an experimental borehole, KLW2, which was constructed in cement concrete with a borehole diameter of 76 mm (Lee et al., 2008). To determine the velocities in the formation, semblance analysis (Kimball and Marzetta, 1984) was applied to sonic data acquired using a measurement system consisting of a transmitter and three receivers. The semblance result (Figure 2) from a monopole source centred at 20 kHz (a) reveals two dominant peak arrivals with velocities of about 3400 m/s and 2000 m/s, which correspond to compressional (P) and shear (S) velocities in the formation, respectively. Another peak arrival with a velocity near 1300 m/s, and arrival time between 800 µs and 950 µs, corresponds to the Stoneley mode (ST). The shear velocity was confirmed by the presence of only one significant flexural peak arrival (Flex) obtained from a dipole source centred at 5 kHz (b). Table 1 shows the physical model parameters for this theoretical model study, based on the compressional and shear velocities described above, and density obtained from core density measurements.

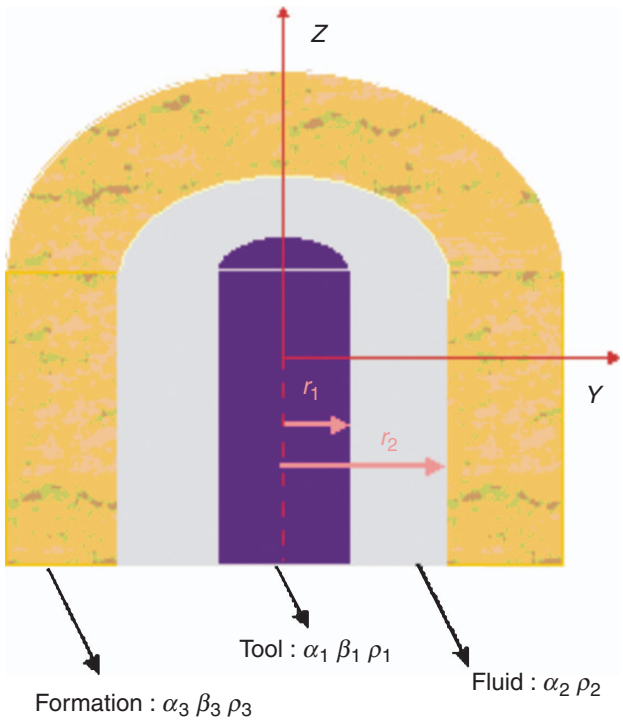

Fig. 1. Schematic diagram of the cylindrical structure of a tool-included fluid-filled borehole.

Presentation of dispersion curves

Dispersion curves from monopole source

The dispersion curves obtained from the Φ520 mm, Φ150 mm, and Φ76 mm boreholes using a monopole source are presented in Figures 3–5: for the tool-absent borehole (a) and the tool-included borehole (b), respectively. Both the phase (solid line) and group (dashed line) velocities of pseudo-Rayleigh (PR) and Stoneley (ST) modes are shown.

Figure 3 exhibits the dispersion curves obtained from the Φ520 mm borehole using a monopole source. The tool-absent (Figure 3*a*) and the tool-included boreholes (Figure 3*b*) show similar dispersion curves, in which more than six pseudo-Rayleigh modes were identified within the frequency range of 30 kHz. All phase velocity curves asymptotically approach formation shear velocity at low frequencies and fluid compressional velocity at high frequencies. The group velocity

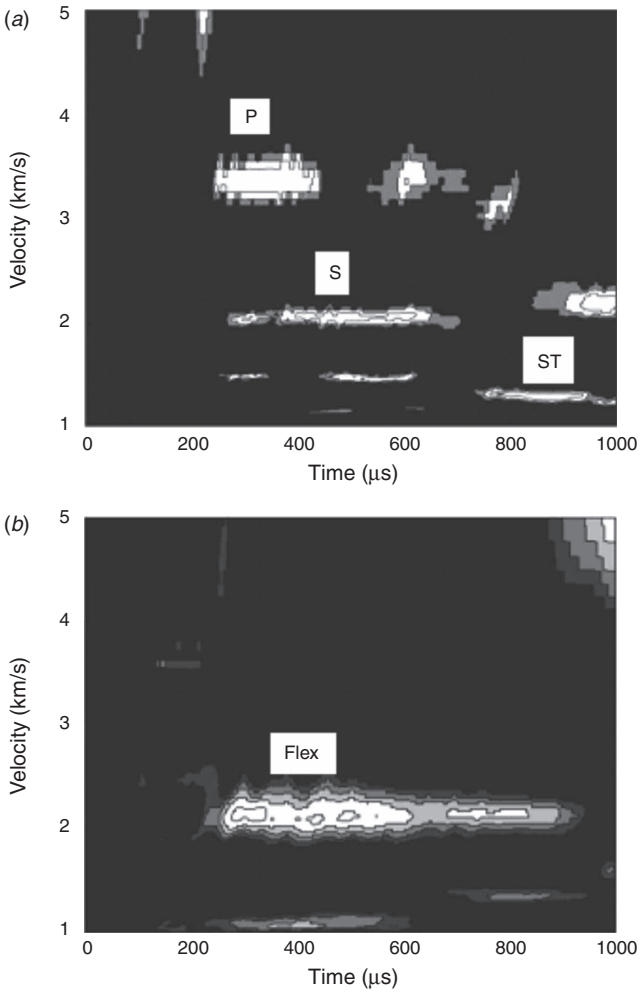

Fig. 2. Semblance result obtained from the experimental borehole KLW2: monopole source (*a*) and dipole source (*b*). Vp, Vs, ST, and Flex denote compressional, shear, Stoneley, and flexural mode arrivals, respectively.

Table 1. Physical parameters of theoretical borehole models. The diameter of the tool is 3.81 cm.

Classification	V_P (α) m/s	V_S (β) m/s	Density (ρ) t/m^3
Tool (1)	6100	3400	7.5
Fluid (2)	1500	0	1.0
Formation (3)	3440	2010	2.2

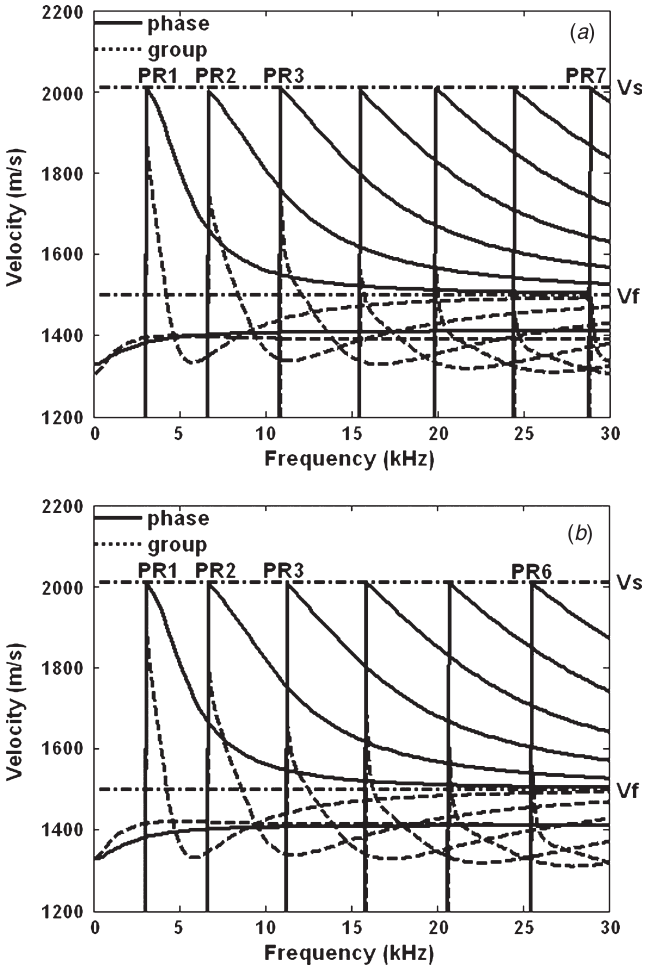

Fig. 3. Dispersion curves obtained from a monopole source in a fluid-filled borehole of Φ520 mm, from tool-absent model (*a*) and tool-included model (*b*). Dashed horizontal lines, marked by V_s and V_f denote the shear velocity in the formation and the compressional velocity in the borehole fluid, respectively. Physical parameters are listed in Table 1.

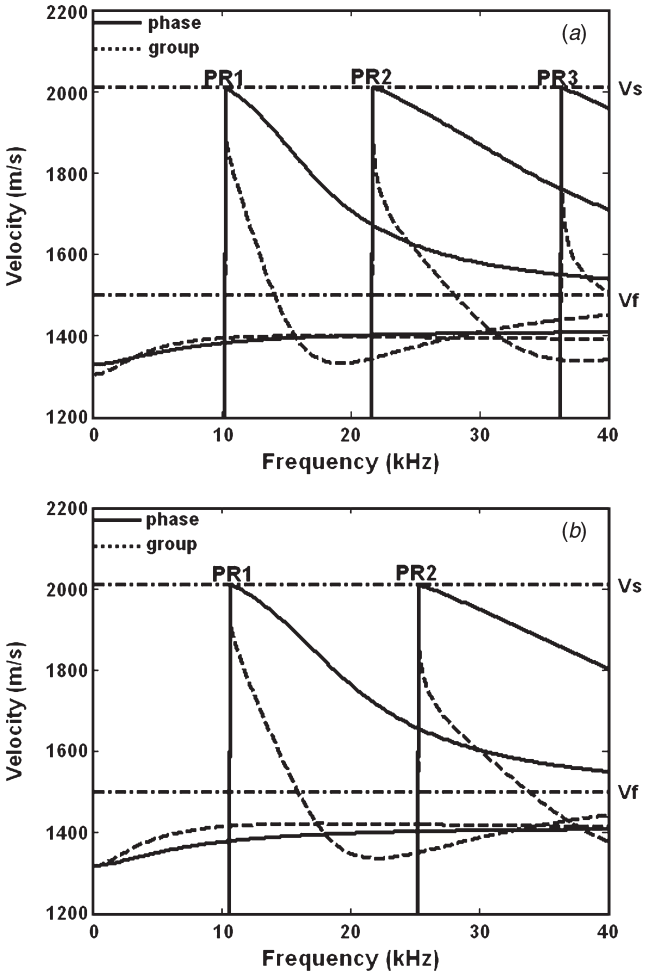

Fig. 4. Dispersion curves obtained from a monopole source in a fluid-filled borehole of Φ150 mm, from tool-absent model (*a*) and tool-included model (*b*). Other explanations are the same as in Figure 3.

of pseudo-Rayleigh mode shows steeper dispersion curves with a significant Airy phase. The Stoneley mode exhibits weak dispersion throughout the frequency range of interest.

Figure 4 shows the dispersion curves obtained from the Φ150 mm borehole using a monopole source. The dispersion curves obtained from the tool-absent borehole (Figure 4*a*) shows three pseudo-Rayleigh modes in the frequency range of 40 kHz. Each phase velocity curve starts at the shear velocity at cut-off frequency and is asymptotic to the fluid wave velocity at high frequencies. The pseudo-Rayleigh mode from the Φ150 mm borehole exhibits gentler dispersion curves compared to the curves obtained from the Φ520 mm borehole. The dispersion curves obtained from the tool-included borehole model (Figure 4*b*) are very similar to those from the tool-absent borehole. The only difference is the slight increase of the cut-off frequency in the pseudo-Rayleigh modes, and correspondingly the 3rd pseudo-Rayleigh mode is not observed within the frequency range of interest.

The monopole-source dispersion curve obtained from the Φ76 mm borehole (Figure 5) shows only one pseudo-Rayleigh mode in the frequency range of 40 kHz, with the phase velocity curve starting at the shear velocity at cut-off frequencies and being asymptotic to the fluid velocity at high frequencies. Both tool-absent (a) and tool-included (b) borehole models revealed similar dispersion curves. The increase of the cut-off frequency and the weakening of the rate of decrease of velocity of the pseudo-Rayleigh mode are shown to be the only difference. In the Stoneley mode, a significant increase of dispersion was observed in the tool-included borehole model.

Dispersion curves from dipole source

For dipole-source responses, dispersion curves are presented for the tool-absent borehole (Figure 6) and the tool-included borehole (Figure 7), and the dispersion curves for each model are shown in the order of Φ520 mm (a), Φ150 mm (b), and Φ76 mm boreholes (c).

The Φ520 mm tool-absent borehole response (Figure 6*a*) exhibited eight flexural modes within the frequency range of 30 kHz. The dispersion curves obtained for Φ150 mm boreholes (Figure 6*b*) consisted of three flexural modes in the frequency range of 40 kHz with gentler dispersion curves compared to the dispersion curves obtained from the Φ520 mm borehole. The Φ76 mm borehole shows only two flexural modes in the frequency range of interest, and a significant increase of cut-off frequency was noted; the first flexural mode at 4 kHz, and the second flexural mode at 26 kHz (Figure 6*c*).

Dipole dispersion curves obtained for the tool-included borehole (Figure 7) reveal faster and slower flexural curves, which correspond to coupled modes (Hsu and Sinha, 1998). Only phase velocities are presented for the borehole sizes of Φ520 mm (a), Φ150 mm (b), and Φ76 mm (c), and it is revealed

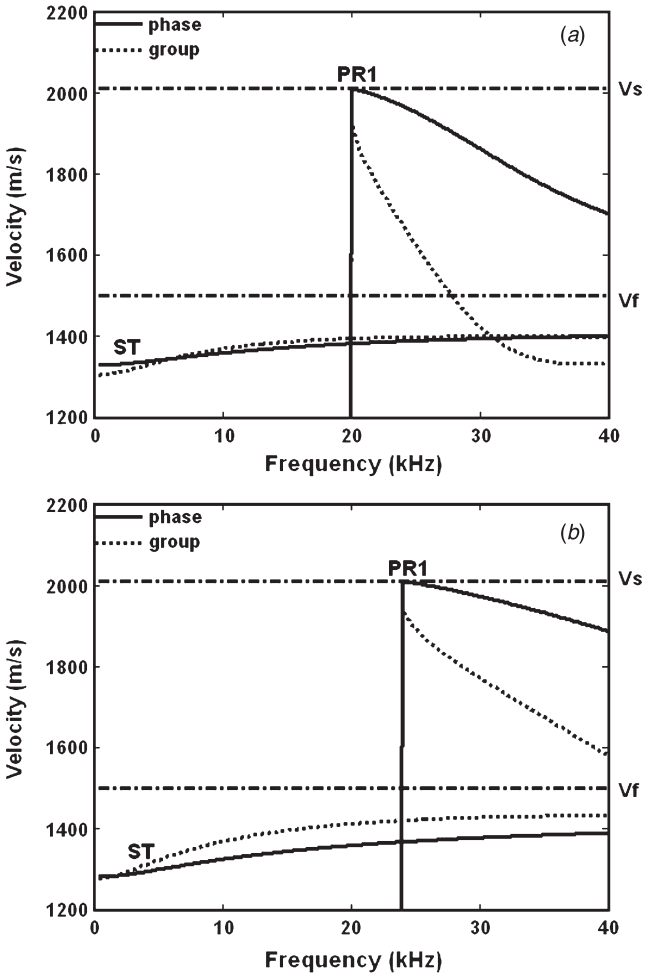

Fig. 5. Dispersion curves obtained from a monopole source in a fluid-filled borehole of Φ76 mm, from tool-absent model (*a*) and tool-included model (*b*). Other explanations are the same as in Figure 3.

that both the faster and slower flexural dispersion curves are complicated by the exchange of dispersion characteristics between tool flexural mode and borehole flexural mode. The faster flexural dispersion curves, asymptotic to formation shear velocity near the cut-off frequency, show a decreasing velocity following the trajectory expected from borehole flexural mode at low frequencies, and then an increase in velocity, roughly following the trajectory expected from tool flexural mode at high frequencies, particularly in small boreholes. By contrast, the slower flexural dispersion curve shows a similar dispersion to that expected for tool flexural mode at low frequencies and for borehole flexural mode at high frequencies.

Borehole size and tool effects

Dispersion curves presented in Figures 3–7 indicate a tendency for increase in cut-off frequency and decrease in the number of pseudo Rayleigh modes in the frequency range of interest with the decrease of borehole size. The tendency of the cut-off frequency to increase is shown well in Figure 8, where the first pseudo-Rayleigh dispersion curves obtained from boreholes of Φ520 mm, Φ150 mm, and of Φ76 mm are compared. Both the tool-absent borehole (a) and the tool-included borehole (b) show the same tendency with the decrease in borehole size; (1) a gentler slope of the dispersion curve and (2) an increase in cut-off frequency.

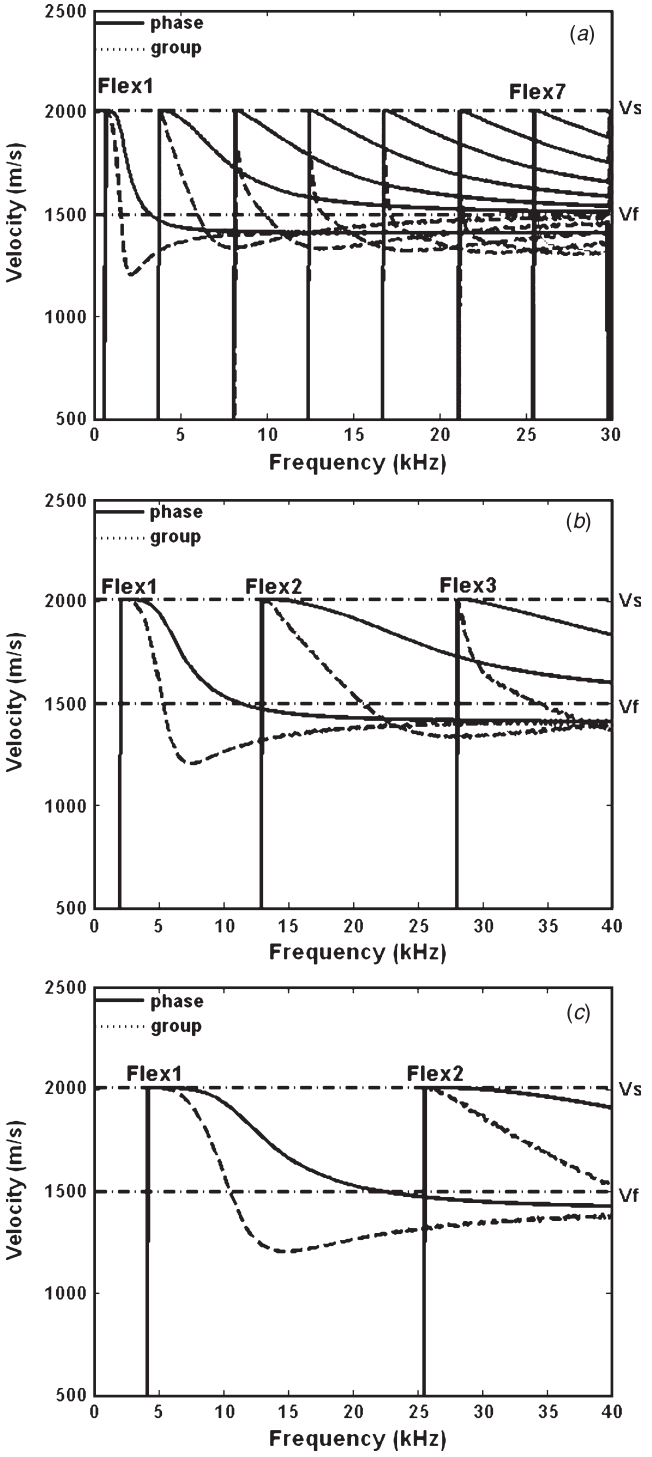

Fig. 6. Flexural dispersion curves obtained from a dipole source in tool-absent boreholes of Φ520 mm (*a*), Φ150 mm (*b*), and Φ76 mm (*c*). Flex_i denotes the ith flexural mode. Other explanations are the same as in Figure 3.

The tendency of the cut-off frequency to increase with the decrease of borehole size is illustrated best in Figure 9, where cut-off frequencies are plotted versus diameter of the model boreholes. To plot Figure 9, additional computation of cut-off frequencies of the first pseudo-Rayleigh and flexural modes were made for borehole models with diameters Φ50 mm, Φ100 mm, Φ200 mm, Φ300 mm, and Φ400 mm.

The pseudo-Rayleigh cut-off frequency versus borehole size plot, for both the tool-absent and the tool-included models (Figure 9*a*) shows a clear tendency for the cut-off frequency to

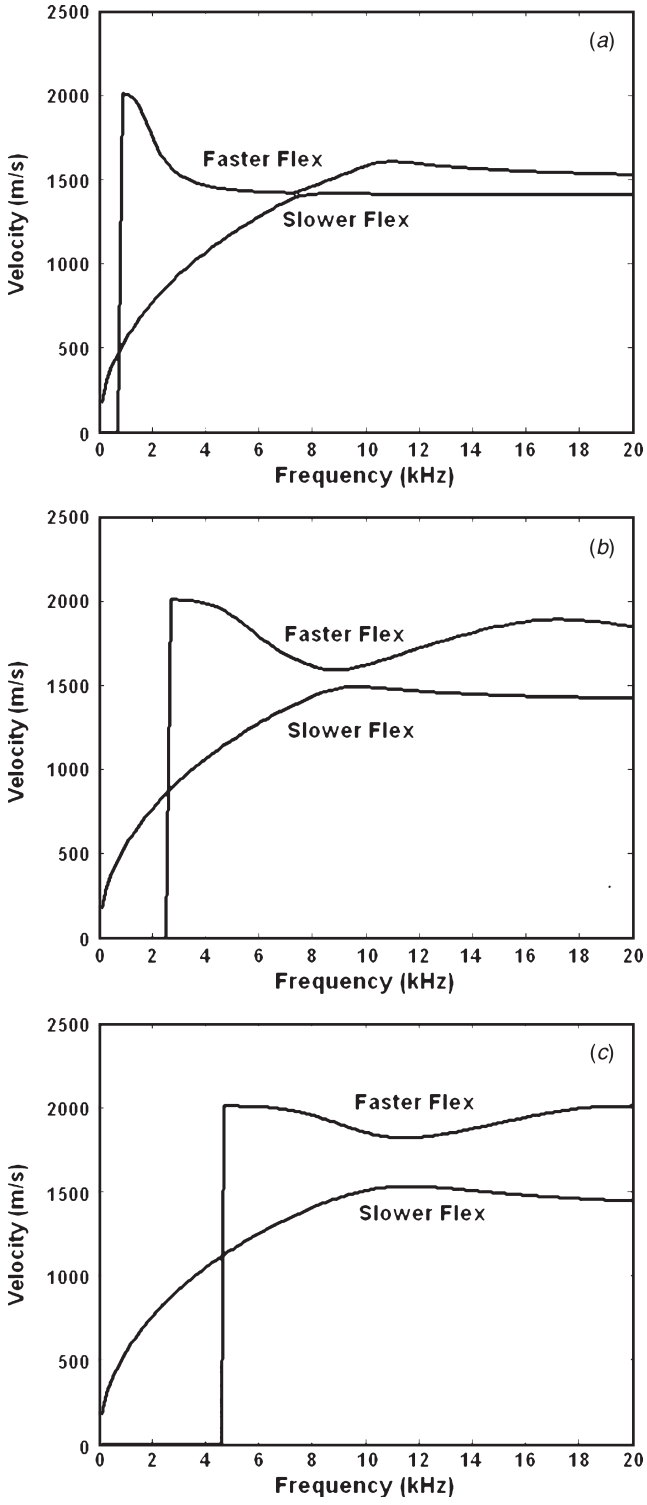

Fig. 7. Dipole phase dispersion curves obtained from tool-included boreholes of Φ520 mm (*a*), Φ150 mm (*b*) and Φ76 mm (*c*). The tool was considered to be a steel rod. Other explanations are the same as in Figure 3.

decrease with increase in borehole size, and each set of data was fitted by an inverse exponential function. The cut-off frequencies from the tool-included models coincide well with the cut-off frequencies from the tool-absent models for diameters greater than 150 mm, whereas significant differences in cut-off frequencies between the tool-included and the tool-absent models was identified in the boreholes of small sizes, particularly at 50 mm and 76 mm in diameter.

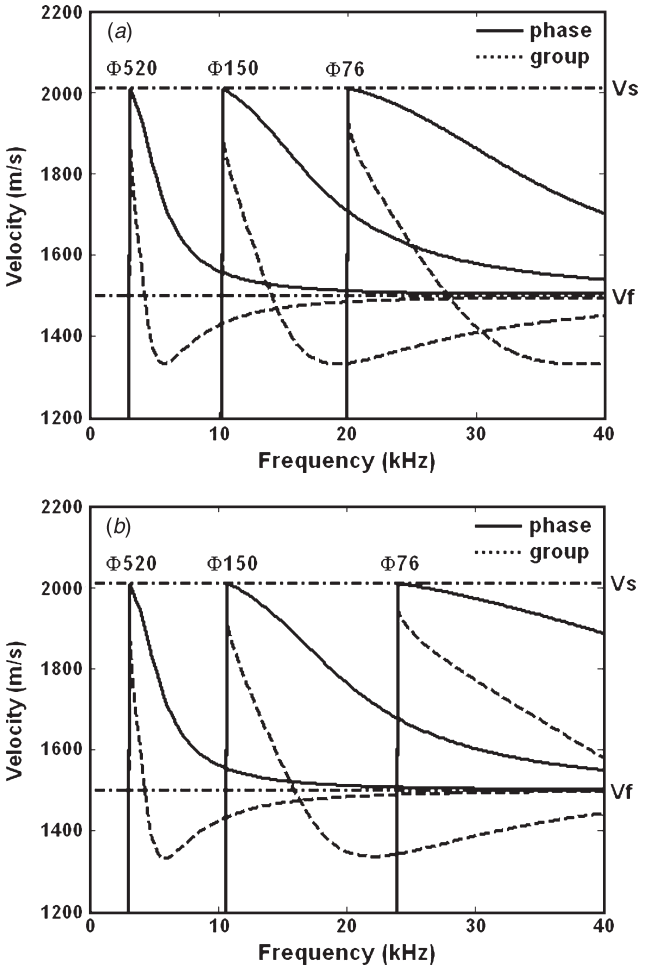

Fig. 8. Variation in dispersion curves of the first pseudo-Rayleigh mode with change of borehole diameters (Φ520, Φ150, and Φ76): from tool-absent (*a*) and tool-included borehole (*b*) models.

The tendency of cut-off frequency to increase with the decrease in borehole size was also shown in the dispersion curves obtained from dipole source (Figure 9*b*), even though the frequency change is limited to less than 7 kHz within the diameter range of interest. When the comparison of cut-off frequencies is made between tool-absent and tool-included, the tool-included boreholes in general show higher cut-off frequencies than the tool-absent boreholes. Although the variation in cut-off frequencies for the flexural mode differs slightly from pseudo-Rayleigh cut-off frequencies, a fairly clean reciprocal relationship between cut-off frequency and borehole size is revealed. It is noted that cut-off frequency is exponentially proportional to the inverse of borehole radius in all cases; for the pseudo-Rayleigh mode, the flexural mode, the tool-absent model, and the tool-included model. Sinha and Asvadurov (2004) reported that the cut-off frequency of the anharmonic mode is inversely proportional to the borehole radius in the absence of any tool. A good correlation was obtained between calculated and fitted values ($R^2 > 0.98$).

For further comparison of dipole-source dispersion characteristics between tool-absent and tool-included models and between different borehole sizes, we overlaid the dispersion curves for tool-included and tool-absent borehole models using the data obtained from boreholes of Φ520 mm and Φ76 mm diameter. Figure 10 shows two pairs of coupled modes; thinner ones from Φ520 mm, and thicker ones from Φ76 mm, which are duplicates of the faster (solid) and the

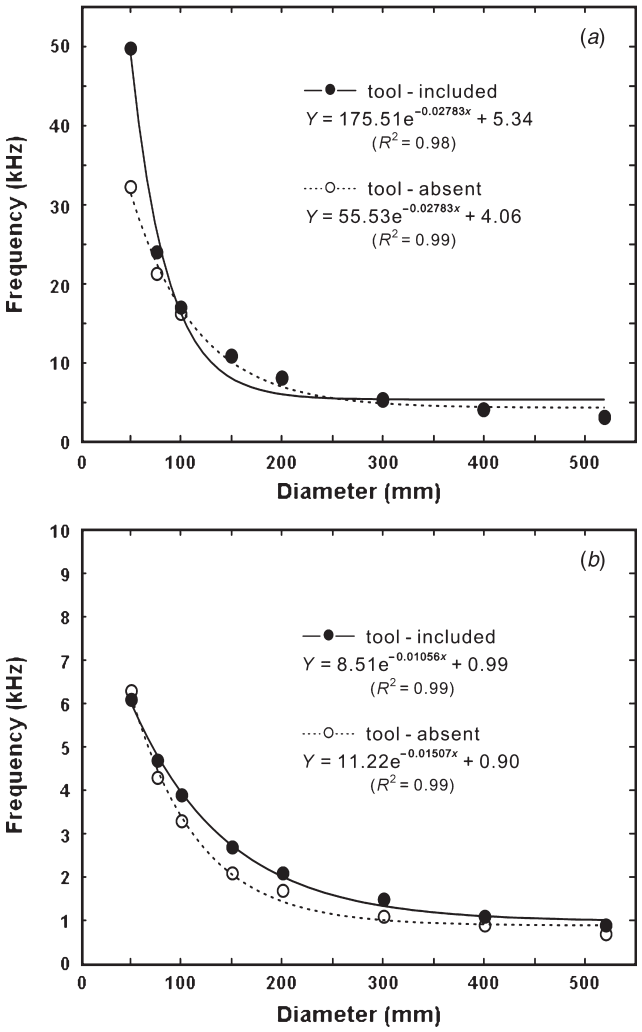

Fig. 9. Crossplot showing the reciprocal relationship between cut-off frequency and borehole diameter, from pseudo-Rayleigh (*a*) and flexural modes (*b*).

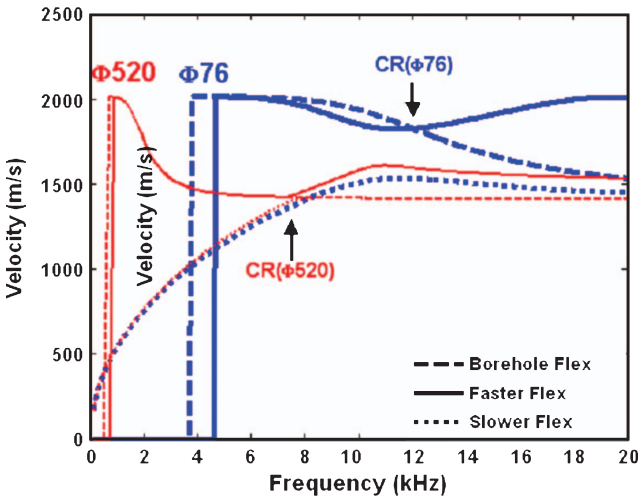

Fig. 10. Comparison of dipole dispersion curves between tool-included (solid line) and tool-absent (dashed line) models using Φ76 mm (thick line) and Φ520 mm (thin line) boreholes. The arrow represents approximately the crossover frequency for each borehole model of different size.

slower (dotted) ones in Figure 7*a* and Figure 7*c*. The first borehole flexural modes are also overlain as dotted lines, which are duplicates of the solid lines in Figure 6*a* and Figure 6*c*. The rod flexural mode presented by Hsu and Sinha (1998) follows approximately the trajectory of the slower and the faster flexural modes in boreholes of Φ76 mm diameter, below and above the cross over frequency.

There is a small bias in cut-off frequencies between the first flexural mode from the tool-absent borehole and the faster flexural mode from the tool-included borehole, irrespective of borehole size. Velocity bias between the first borehole flexural curve and the faster flexural curve before the crossover frequency is also very small, particularly in the Φ520 mm borehole. In the Φ520 mm borehole model, the borehole flexural curve coincides precisely with the faster flexural curve and the slower flexural curve before and after the crossover, respectively. Note that the tool flexural mode and the first flexural mode interact at the region near 11 kHz in the Φ76 mm borehole, and 7.5 kHz in the Φ520 mm borehole. They exchange dispersion characteristics, and both faster and slower flexural curves were divided into two segments with the boundary of each crossover frequency. Although faster flexural curves increase again to the level of the formation shear velocity at high frequencies after the crossover frequencies, it is considered to be a coincidence due to the similarity between the formation shear and the rod flexural mode velocities.

The velocity separation between the two coupled modes is greater than the separation between two uncoupled modes at all frequencies, as was reported by Hsu and Sinha (1998), and the velocity separation is shown to increase with the decrease in borehole size. Hsu and Sinha (1998) reported that the tool effect will be significant if the tool flexural mode dispersion is not well separated from the borehole flexural dispersion at all frequencies of interest. From this point of view, the increase of separation in velocity between the two dispersions, as well as the wider range over which the faster flexural mode is asymptotic to formation shear velocity in an engineering borehole, can be a favourable condition for determining formation shear velocity while excluding tool effects. In addition, the presence of an acoustic isolator between the transmitter and an array of receivers significantly mitigates the excitation of any such tool modes (Sinha and Asvadurov, 2004). Consequently, it is expected that formation shear velocity determination will not be significantly disturbed by the presence of a sonic tool.

Conclusions

A series of theoretical dispersion curves were computed from three borehole models having the same physical properties, determined from an experimental borehole KLW2, but different borehole sizes of Φ520 mm, Φ150 mm, and Φ76 mm. Comparisons and analyses were made between boreholes of different sizes and between tool-absent and tool-included models.

Between tool-included and tool-absent boreholes, substantial similarities and significant differences were shown for monopole and dipole sources, respectively: monopole-excited pseudo-Rayleigh modes showed similar dispersion curves with a tendency for the number of modes to decrease and a gentler slope, irrespective of the existence of a tool, whereas dipole-excited flexural modes exhibited a significant difference between tool-absent and tool-included boreholes. Dispersion curves obtained for the dipole source in a tool-included borehole were characterised by faster flexural and slower flexural curves. The faster and the slower flexural curves, below the crossover frequencies, are close to the uncoupled borehole and the tool flexural modes, irrespective of borehole sizes. Above the crossover frequencies, the faster and the slower flexural curves

pass through a region between two trajectories expected for uncoupled tool and borehole modes. It was noted that the faster flexural curves above the crossover frequencies move closer to the uncoupled borehole flexural curves with the increase in borehole size. Correspondingly, it seems that dispersion curves above the crossover frequencies for the tool-included boreholes follow the dispersion properties of uncoupled borehole flexural modes as borehole sizes increase.

Dispersion curves exhibited a tendency for cut-off frequency to increase with decreasing borehole size, as indicated by previous studies (Hsu and Sinha, 1998; Rao et al., 1999). This was common to both monopole-source pseudo-Rayleigh and dipole-source flexural modes in the frequency range of interest, and for both the tool-absent and the tool-included models as well. In this study, we have confirmed that the cut-off frequency is exponentially proportional to the inverse of borehole radius, irrespective of mode type and of the existence of a tool in the borehole. Cut-off frequencies could be expressed as an exponential function of the inverse of the borehole radius with a good correlation rather than the previous general recognition of an inversely proportional relationship between cut-off frequency and borehole radius.

In this comparative study, borehole size and tool effects on the dispersion properties of sonic waves have been revealed more clearly than in previous studies, which did present the dispersion characteristics for each borehole environment well, and the result was helpful in understanding the dispersion characteristics for various borehole environments.

Acknowledgments

The authors express sincere thanks to Mr. Sungkun Park and Byoung Chol Hwang of Kangwon National University for much help in writing this paper. We are indebted to the anonymous referees for their valuable comments and suggestions on this paper.

References

Aki, K., and Richards, P. G., 1980, *Quantitative seismology theory and methods*, **1**, W.H. Freeman and Company, 556.

Biot, M. A., 1952, Propagation of elastic waves in a cylindrical bore containing a fluid: *Journal of Applied Physics*, **23**, 997–1005. doi: 10.1063/1.1702365

Cheng, C. H., and Toksöz, M. N., 1981, Elastic wave propagation in a fluid-filled borehole and synthetic acoustic logs: *Geophysics*, **46**, 1042–1053. doi: 10.1190/1.1441242

Hsu, C., and Sinha, B. K., 1998, Mandrel effects on the dipole flexural mode in a borehole: *Journal of the Acoustical Society of America*, **104**, 2025–2039. doi: 10.1121/1.423767

Kimball, C. V., and Marzetta, T. L., 1984, Semblance processing of borehole acoustic array data: *Geophysics*, **49**, 274–281. doi: 10.1190/1.1441659

Kurkjian, A. L., and Chang, S., 1986, Acoustic multipole sources in fluid-filled boreholes: *Geophysics*, **51**, 148–163. doi: 10.1190/1.1442028

Lee, S., Kim, Y., and Hwang, B. C., 2008, An experimental study on log correction for plastic cased slim boreholes: *Journal of Korean Society of Engineering Geology*, **18**, 137–144.

Paillet, F. L., and Cheng, C. H., 1991, *Acoustic waves in boreholes*, CRC press, 264.

Paillet, F. L., and White, J. E., 1982, Acoustic modes of propagation in the borehole and their relationship to rock properties: *Geophysics*, **47**, 1215–1228. doi: 10.1190/1.1441384

Rao, V. N. R., Burns, D. R., and Toksoz, M. N., 1999, Models in LWD applications, M.I.T., Earth Resources Laboratory Annual Report, 5–14.

Rao, V. N., Zhu, Z., Burns, D. R., and Toksoz, M. N., 2002, Acoustic logging while drilling (LWD): Experimental Studies with Anisotropic media, M.I.T. Earth Resources Laboratory Annual Report, 18.

Sinha, B. K., and Asvadurov, S., 2004, Dispersion and radial depth of investigation of borehole modes: *Geophysical Prospecting*, **52**, 271–286. doi: 10.1111/j.1365-2478.2004.00415.x

Zhao, W., 2008, *Numerical experiments on full waveform logging in slim boreholes*, Ph.D. thesis, Kangwon National University. 125.

Manuscript received 14 November 2008; revised manuscript received 24 December 2008.

시추공경과 공내검층기가 분산곡선에 미치는 영향에 대한 비교 연구

조유준[1], 김종만[2], 김영화[2]

1 토호쿠대학교 북동아시아 연구센터
2 강원대학교 지구물리학과

요 약 : 단극 및 쌍극 음원을 이용하여 S파속도 결정에 큰 영향을 미치는 분산특성을 연구하였다. 이를 위하여 동일한 물성을 가지면서 공경을 달리하는 3종류의 시추공모형(Φ520 mm. Φ150 mm, and Φ76 mm)을 중심으로 이론 분산곡선을 구하고 공경과 공내검층기 존재 유무에 따른 분산 특성의 변화를 비교 분석하였다. 분산곡선의 형태 는 단극음원에서 시추공 내의 공내검층기 유무에 크게 영향을 받지 않고 비슷하게 나타난 반면에 쌍극음원에서는 공내검층기 유무가 큰 차이를 보였다. 반면에 절단주파수에서는 쌍극음원에 비하여 단극음원에서 공내검층기 유무에 따른 차이가 크며 특히 소구경 시추공에서 큰 차이를 보여 단극음원을 이용한 토목시추공 음파검층에서 주파수 선택이 매우 중요한 변수가 될 수 있음을 보였다. 수치모델링결과, 절단주파수와 시추공경과의 관계는 기존에 알려진 일반적인 반비례 관계보다는 지수함수적으로 감소하는 관계임을 확인하였으며, 분산모드의 종류나 공내검층기 유무에 상관없이 각 환경에 있어서의 절단주파수 값을 지수함수로 표시할 수 있었다. 특정 시추공 환경에서의 분산곡선 및 분산특성들은 과거 연구결과들로부터 비교적 잘 알려져 있지만 분산곡선의 직접 비교에 의하여 분산특성에 미치는 시추공경과 공내측정기 영향을 보다 구체적으로 밝힐 수 있었다.

주요어 : 분산, 단극음원 및 쌍극음원, 공경, 검층봉 영향, 절단주파수

坑径と坑井ツールが分散曲線に及ぼす影響の比較研究

趙維俊[1]・金鐘萬[2]・金永和[2]

1 東北大学 東北アジア研究センター
2 江原大学 地球物理学部

要　旨 : 音波検層の分散特性は、最も重要な研究対象の一つであり、とりわけS波の速度を評価する際に重要である。我々は、モノポール震源とダイポール震源を使用して分散特性を分析した。理論的な分散曲線を坑井ツールの有り無しのそれぞれの場合において、物性は同じであるが異なる坑径（Φ520 mm, Φ150 mm, Φ76 mm）の条件のもとで計算した。すなわち、坑径の違いと坑井ツールの有無による比較をした。坑井ツールの有無において、モノポール震源の場合には非常に似た分散曲線が示され、ダイポール震源の場合には著しく異なった曲線が示された。しかしながら、とりわけ土木用の坑井（Φ76 mm and Φ50 mm）においてモノポール震源からの信号に対して、カット・オフ周波数の著しい相違が確認されたが、ほぼ同様のカット・オフ周波数がダイポール震源の場合にも認められた。このことは、土木用の坑井においては、モノポール震源の周波数の選択をする際は、十分注意する必要があることを意味する。

数値実験の結果によれば、カット・オフ周波数は坑径の逆数に指数関数的に比例し、震源モードや坑井ツールの有無によらないことを示した。さらに、それぞれの坑井環境に対するカット・オフ周波数は、以前一般的に認識されたようなカット・オフ周波数と坑径との間の逆比例関係というより、むしろ指数関数として表現されることを示した。分散曲線を直接比較することにより、坑径と坑井ツールの分散特性への影響は、坑井環境と分散特性を別々に扱っている従来の研究と比較して、より明確に示すことができる。

キーワード : 分散，モノポール・ダイポール震源，坑径，坑井ツール効果，カット・オフ周波数